Nanoscale architecture

Hazelaar, Sandra

Chapter **3**

Ubiquitination of cell wall associated proteins during valve formation of *Navicula pelliculosa* (Bacillariophyceae): implications for micromorphogenesis

Sandra Hazelaar, Han J. van der Strate, Winfried W.C. Gieskes & Engel G. Vrieling

Abstract

In *Navicula pelliculosa* (Brébisson et Kützing) Hilse a homologue of the conserved protein ubiquitin has been found that appears to accumulate in the very proximity of the siliceous parts of the cell wall during valve formation in Si-synchronized cells. Here we demonstrate that levels of poly-ubiquitins and ubiquitinated proteins in this species change over time in the course of valve formation. Most striking is that during valve formation the level of 7 soluble and 7 cell wall-associated ubiquitinated proteins fitted significantly to second order polynomial correlations. A clear difference was observed between the amount of ubiquitinated proteins in the first 120 min of valve formation and the following period up to 8 hrs, indicative of a well-timed ubiquitination event for these proteins. The anti-ubiquitin labeling intensity of these proteins rapidly increased – except for a 48 kDa protein in the EDTA-extracts – at the early stage of valve formation (< 120 min). Typically, the contribution of larger cell wall-associated ubiquitinated proteins (> 50 kDa) appeared to increase in this same period, followed by a decline indicating that they were processed in the period > 90 min. The timing of this ubiquitination event agrees well with the rapid 2D valve formation earlier described for a closely related species. Our results imply that the ubiquitination machinery contributes to diatom valve formation, and we suggest that it is involved as part of the valve micromorphogenesis, that is steered by phase separation processes that include removal of protein-rich phases upon completion of the silica of the valves.

Introduction

In spite of long-standing efforts the molecular and physico-chemical principles involved in the biogenesis of the siliceous cell wall, the frustule, of diatoms remain elusive (Gordon & Drum 1994; Pickett-Heaps *et al.* 1990; Müller 2003). Proteins seem to play a central role at various stages of valve formation. Silicon transport proteins (SITs) have been identified to play a key role in uptake of silicic acid from the environment and transporting it across membranes (Hildebrand *et al.* 1997). Each of the 5 SITs of *Cylindrotheca fusiformis* Reimann et Lewin differs with respect to its transport affinity and/or capacity (Hildebrand *et al.* 1998; Hildebrand 2003), but their exact role in diatom biosilica formation has not been fully determined yet (Thamatrakoln & Hildebrand 2004). Casing proteins that have been identified are frustulins and pleuralins, all located at the surface of the frustules (Kröger *et al.* 1994; 1996; 1997; van de Poll *et al.* 1999; Kröger & Wetherbee 2000). Based on their expression and distinct localization, frustulins appear to be associated with the organic casing that is formed when siliceous parts are completed (van de Poll *et al.* 1999). Pleuralins of *C. fusiformis* are confined specifically to the sites where girdle bands are interconnected by pleural girdle bands (Kröger & Wetherbee 2000).

Also silaffins and long-chain polyamines (LCPAs), extracted following fluoride-based silica dissolution, have been identified and characterized for activity in *in vitro* silica precipitation (Kröger *et al.* 1999; 2002; Poulsen *et al.* 2003; Sumper & Kröger 2004; Wong Po Foo *et al.* 2004). Especially the native peptide natSil-1 and LCPAs induce silica precipitation, and when mixtures of these compounds (eventually with natSil-2 included) are used a variety of silica structures is formed (Sumper & Kröger 2004).

The identification of silaffins and LCPAs has been the basis of two different models that describe phase-separation processes as the mechanism of structure-directed formation and hierarchical ordering of pores in diatom biosilica. The computational model of Sumper (2002) involves a repetitive, down-scaling, mechanism controlled by phase separation processes, in which the sequential steps lead to formation of large pores downwards to the smallest ones. On the other hand, the experimentally-based *cire perdu* model of Vrieling *et al.* (2002) implies an up-scaling mechanism controlled also by phase separation processes, as demonstrated for silica syntheses in the presence of proteins and organic polymers (Sun *et al.* 2002; 2004). Phase separation processes induced by organic molecules lead to discrimination of silica-rich and organic-rich phases (Vrieling *et al.* 2002; Sun *et al.* 2002; 2004). Subsequently, these protein-rich phases may become trapped as enclosures in the silica-rich phase, which solidifies to amorphous silica. When this protein-rich phase is removed, the cavities would remain as the characteristic mesopores in the frustule, as in calcination of artificially produced silicas (Vrieling *et al.* 2003; 2005). So far, the removal processes in diatoms proposed by Vrieling *et al.* (2002) were purely speculative.

In our search for proteins involved in diatom valve formation, we recently have identified a ubiquitin homologue in the pennate species *Navicula pelliculosa* (Hazelaar *et al.* 2003) that as part of the protein degradation machinery may well be involved in the removal of protein-rich phases as described in the aforementioned up-scaling model. Ubiquitin is a highly conserved small (~8.5 kDa) protein that is well known for its role in degradation of short-lived proteins (Hershko & Ciechanover 1998; Hochstrasser 1996; Pickart 2000). Ubiquitin attaches to proteins that are targeted for degradation by a covalent bond between glycine residues at the C-terminal ends of ubiquitin and the lysine residues of the target protein (Hershko & Ciechanover 1998; Hochstrasser 1995); the binding is reversible. A multi-enzymatic pathway links ubiquitin to each other forming a polyubiquitin chain, resulting in poly-ubiquitination of the target protein (Vierstra 1996; Tanaka 1998; Pickart 2000). After our identification of ubiquitin in diatoms, the question arose whether or not this protein degradation machinery is really involved in diatom valve formation. To investigate this, we examined the levels of (poly)ubiquitins and ubiquitinated proteins during valve formation in *N. pelliculosa*, focusing on soluble and cell wall-associated proteins.

Materials and methods

Cultures and growth conditions

Four unialgal mass cultures of 20 L of the benthic pennate diatom *Navicula pelliculosa* (strain CCMP543) were established under equal conditions in artificial seawater with a salinity of 32.5 practical salinity units (PSU; Veldhuis & Admiraal 1987), except that the final concentrations of Na_2SiO_3 9 H_2O and KNO_3 was 0.1 mM and 0.68 mM, respectively. Only the 3 vitamins thiamine hydrochlorid, biotin and cyanocobalamin were added in finals concentration of 296.5 nM, 2 nM, and 0.37 nM, respectively. The mass cultures were inoculated with an exponentially growing pre-culture (grown in 6× 2 L-Fernbach flasks) and incubated for 11 days under continuous aeration at 16°C under a 16:8 h LD cycle, and a light intensity of ~ 60 μmol photons·m^{-2}·s^{-1} (fluorescent tubes, Osram Biolux, Germany). At days 3, 7, and 11 nutrients, trace elements, and vitamins were again added to each vial in order to prevent that the cells would suffer from nutrient limitation. At day 11 the airflow was stopped and the culture was allowed to sediment for 2 days. Sedimented cells were harvested by decanting the culture medium, followed by mild centrifugation (10 min, 1000 x g, 15°C). Subsequently, the cells were washed once with artificial seawater free of silicic acid and resuspended in a volume of 1.7 L Si-free medium. The cells were divided over fifteen 1 L polycarbonate bottles (Nalgene, Neerijse, Belgium) by adding 100 ml of the cell concentrate to 900 ml Si-free medium. To establish cytokinetic arrest induced by silicon limitation (Coombs & Volcani 1968), the cells were incubated for 50 h under the aforementioned conditions. Synchronized growth was initiated in 14 bottles by repleting the culture with silicic acid at a final concentration of 0.15 mM. Also KNO_3, NH_4Cl, and $NaH_2PO_4 \cdot H_2O$ were added to final concentrations of 0.34 mM, 24.8 mM, and 18 mM, respectively; one bottle was processed before silicon addition to harvest cells in cytokinetic arrest (this sample is denoted as t = 0). Directly following resupply of silicic acid, the bottles were sequentially processed to harvest the cells by centrifugation (5 min, 10,000 x g, 0°C). The centrifugation time was incorporated in the harvesting times assuming that valve formation continuous during centrifugation. This led to final harvesting times of 5, 10, 15, 20, 25, 30, 40, 50, 60, 90, 120, 240, 360, and 480 min after resupply of silicic acid. This time frame is needed to complete one cell division (van de Poll *et al.* 1999). Pelleted cells were quickly transferred to a 50 mL plastic tube, immediately frozen in liquid nitrogen, and stored at –20°C until they were freeze-dried.

Cell fractionation

Equal amounts of freeze-dried cell pellets (0.4 g) were used for every interval harvested, and suspended in 40 mL 1 mM $CaCl_2$, in addition of 1.6 mL Complete Protease Inhibitor Cocktail (Roche Applied Science, Indianapolis, USA) and 0.4 mL 100 mM phenylmethylsulfonylfluoride (PMSF). The pellets were disrupted by

adding 1 g glass beads and vortexing the samples six times for 1 min, putting them 4 min on ice in between vortexing. The disrupted cells were centrifuged (10 min, 2000 x g, 4°C) and the supernatants, further denoted as cell free extracts, were collected and freeze-dried. The pellets containing the cell walls and other cell debris were separated from the glass beads by resuspension in 40 mL 1 mM $CaCl_2$, leaving the glass beads to sink quickly to the bottom and immediately pouring the solution into a new tube. These samples containing cell walls and debris were washed thoroughly with 40 mL 1 mM $CaCl_2$ using 12 centrifugation cycles (10 min, 650 x g, 4°C). After this washing procedure nearly all cellular matter was removed, leaving highly enriched cell wall fractions for further extraction. These cell wall fractions were first extracted in 40 mL 100 mM EDTA (pH 8; Kröger *et al.* 1994), incubated overnight on a shaker at 4°C, and than centrifuged (10 min, 2000 x g, 4°C) to collect the supernatant. The cell walls were washed with 40 mL MilliQ water, again centrifuged (10 min, 2000 x g, 4°C), and the supernatants were pooled with the EDTA supernatant obtained earlier. This final EDTA-extract of each interval was freeze-dried and stored at -20°C until further analysis. The EDTA-extracted cell walls were resuspended in 40 mL 10 mM Tris-HCl buffer (pH 6.8) containing 1% (w/v) SDS and heated for 1 h at 95°C in a water bath (Kröger *et al.* 1997). Subsequently, the supernatant was collected following centrifugation (10 min, 2000 x g, 4°C) and the extracted cell walls were washed once with 40 mL MilliQ water, again centrifuged and the supernatants were pooled with the first SDS-extracts. These final SDS-extracts were also freeze-dried and stored at -20°C until further analysis.

Protein analysis

All freeze-dried extracts (cell free-, EDTA-, and SDS-extracts) were resuspended in 2 mL MilliQ water, vortexed gently to dissolve the pellets, and centrifuged shortly (3000 x g, 4°C) to remove insoluble matter. Protein concentrations were determined for all cell free- and EDTA- extracts after freeze-drying, using a protein assay (Biorad, Hercules, USA) based on the method of Bradford (1976). Similarly, the protein concentrations in the SDS extracts were analyzed, but in this case the RC DC protein assay (Biorad, Hercules, USA) was used that is based on the protocol by Lowry *et al.* (1951).

Protein separation and Western blotting

From all extracts salts were removed using microconcentrators (Millipore, Bedford, USA) with a 3 kDa cut-off. Of each cell free- and SDS-extract 15 μL sample was heated together with 15 μL of SDS sample buffer (Laemmli 1970) at approximately 96°C for 5 min. Of each EDTA-extract 30 μL was heated together with 30 μL of sample buffer. Afterwards the proteins were separated by SDS-PAGE according to Laemmli (1970), using polyacrylamide percentages of 10% (w/v) and a Mini Protean III System (Biorad, Hercules, USA).

Following SDS-PAGE, the separated proteins were semi-dry blotted on a PVDF membrane according to Kyhse-Anderson (1984). The blots were washed with Tris-buffered-saline (TBS) and blocked for 1 h in blocking buffer (TBS containing 5% (w/v) milk powder). After blocking, the blots were washed three times for 5 min with TBS containing 0.05% (v/v) Tween 20 (TBST). The blots were incubated for 2.5 h at room temperature (RT) with sheep anti-ubiquitin (Abcam, Cambridge, UK) at a 1:1500 dilution in blocking buffer, washed three times 10 min with TBST, incubated for 90 min (RT) with a 1:1000 dilution of rabbit anti-sheep IgG conjugated with alkaline phosphatase (Abcam, Cambridge, UK) in blocking buffer, and finally washed three times 10 min with TBST and two times 5 min with 1.3 M Tris (pH 9.5) containing 0.1 M NaCl and 5 mM MgCl2. Directly thereafter, the labeled proteins were stained using a BCIP/NBT solution (Roche, Mannheim, Germany); staining was stopped by a stop buffer of 26 mM Tris (pH 8), containing 3.9 mM EDTA and before drying the blots were washed 2 times for 5 min with MilliQ water. Ubiquitin from bovine red blood cells (Sigma-Aldrich, Zwijndrecht, The Netherlands) was used to confirm labeling (Hazelaar *et al.* 2003). The labeling intensity of each stained protein band was quantified using ImageQuant 4.2 (Molecular Dynamics inc., Sunnyvale, USA), using identical samples present on the blots as an internal reference to normalize the intensity of the proteins bands on the different blots per extract.

Transmission electron microscopy and immunocytochemistry

Transmission electron microscopy was done as described previously (van de Poll *et al.* 1999; Hazelaar *et al.* 2003), in short: ultra thin sections of UNICRYLL™ (BioCell, Cardiff, United kingdom) embedded cells of synchronized *N. pelliculosa* cells were collected on Formvar-coated nickel grids and labeled according to Slot and Geuze (1984). The sections were blocked for 10 min with 0.5% (w/v) BSA in phosphate-buffered saline containing 10 mM glycine (PBSG) and incubated overnight (4°C) with anti-ubiquitin at a 1:100 dilution in PBSG with 0.5% (w/v) BSA. After incubation with the primary antibody, the sections were washed three times for 5 min with PBSG and 1 h incubated (RT) with a 1:10 PBSG-diluted rabbit anti-sheep IgG conjugated with 15 nm gold particles (Aurion, Wageningen, NL). Then the sections were washed six times for 5 min with PBSG, four times 5 min with double-distilled water (ddH_2O), and stained. For staining the sections were incubated 2 min at RT with 1% (w/v) EDTA (pH 4), washed three times 1 min with ddH_2O, and incubated 4 min with 2% (w/v) uranyl acetate. The uranyl-stained sections were subsequently washed three times with ddH_2O, incubated 30 sec with lead citrate (Reynolds 1963), and washed again four times 1 min with ddH_2O. In controls, ultra thin sections were treated similarly, but the primary antibody was omitted. All labeled and stained sections were air-dried prior to examination in a Philips CM10 electron microscope.

DNA sequencing

Based on the N-terminal protein sequence that was obtained earlier (Hazelaar *et al.* 2003), a degenerate primer was developed (5'ATGCARATHTTYGTNAARAC3'). The cDNA sequence data (140 bp) acquired with the degenerate primer using the SMART™ RACE cDNA Amplification kit (BD Biosciences Clontech, USA) was compared using BLAST (Altschul et. al. 1990). It showed high homology with ubiquitin ($1e^{-31}$ with *Aspergillus nidulans*). Based on this cDNA sequence four specific primers (5'CGAGCCCTCGGACACCATCGAC3', 5'CCCGCGAAGATCAAACGCTG CT3', 5'CCGCACTCTCAGCGACTACAACATCC3' and 5'GCTGCTTACCCGCGAA GATCAAACG3') could be designed to obtain a full length copy of *N. pelliculosa* ubiquitin using 3' as well as 5' SMART™ RACE PCR reactions. Multiple sequence alignments were performed using Clustal W 1.82 (Chenna *et al.* 2003) and a Blossum matrix.

Statistics

In each extract a Wilcoxon ranks sum test (significant when p-value < 0.05) was performed for all samples to test whether the levels of positively identified ubiquitinated proteins at the early stages of valve formation ($t < 60$ min) were significantly different to those at the stages beyond ($t > 60$ min). Regression analysis, fitting second order polynomial functions ($\alpha = 0.05$) was also performed for every extract in order to correlate the levels of the anti-ubiquitin labeled proteins to the timing of valve formation.

Results

The presence of ubiquitin in *N. pelliculosa* was confirmed after having obtained the entire DNA sequence of ubiquitin (accession number AY862433; Fig. 3.1A). The cDNA sequence revealed tandem repeats of ubiquitin. A single copy contained 76 amino acids (Fig. 3.1B), the first 16 amino acids exactly match the 16 amino acids earlier obtained by N-terminal sequencing (Hazelaar *et al.* 2003). The cDNA identified was compared using BLAST of the NCBI database (Altschul *et al.* 1997) and results from this search revealed a significant hit with ubiquitin from different organisms (E-values ranging from $1e^{-51}$ to $5e^{-38}$), stating its conservation among many organisms as also becomes clear from an alignment (Fig. 3.1B). This homology suggests that the known ubiquitin functions also apply with respect to those in our diatom.

Transmission electron microscopy revealed a clear and specific labeling of anti-ubiquitin (Fig. 3.2). In negative controls, gold particles were absent (Fig. 3.2A). As earlier demonstrated (Hazelaar *et al.* 2003), ubiquitin was again localized randomly over the cell with gold particles scattered over the cytoplasm and organelles (Fig. 3.2B). Interestingly, however, the labeling was predominantly localized in the very

(A)

```
                                10        20        30        40
                       ....|....|....|....|....|....|....|....|
N. pelliculosa ubiquitin cttcgcgggtaagcagctcgaggacggccgcactctcagc

                                50        60        70        80
                       ....|....|....|....|....|....|....|....|
N. pelliculosa ubiquitin gactacaacatccagaaggaaagcaccttgcatttggtgt

                                90        100       110       120
                       ....|....|....|....|....|....|....|....|
N. pelliculosa ubiquitin tgcgtcttcgcggaggtatgcagatcttcgtcaagacctt

                                130       140       150       160
                       ....|....|....|....|....|....|....|....|
N. pelliculosa ubiquitin gacgggaaagacgatcaccctcgatgtcgagccctcggac

                                170       180       190       200
                       ....|....|....|....|....|....|....|....|
N. pelliculosa ubiquitin accatcgacaacgtcaagaccaagatccaggacaaggaag

                                210       220       230       240
                       ....|....|....|....|....|....|....|....|
N. pelliculosa ubiquitin gtatccctcctgatcagcagcgtttgatcttcgcgggtaa

                                250       260       270       280
                       ....|....|....|....|....|....|....|....|
N. pelliculosa ubiquitin gcagctcgaggacggccgcactctcagcgactacaacatc

                                290       300       310       320
                       ....|....|....|....|....|....|....|....|
N. pelliculosa ubiquitin cagaaggaaagcaccttgcatttggtgttgcgtcttcgcg

                                330       340       350       360
                       ....|....|....|....|....|....|....|....|
N. pelliculosa ubiquitin gaggtatgcagatcttcgtcaagaccttgacgggaaagac
```

(B)

```
NAVPE    MQIFVKTLTGKTITLDVEPSDTIDNVKTKIQDKEGIPPDQQRLIFAGKQL
DROME    MQIFVKTLTGKTITLDVEPSDTTENVKTKIQDKEGIPPDQQRLIFAGKQL
HOMSA    MQIFVKTLTGKTITLDVEPSDTIENVKTKIQDKEGIPPDQQRLIFAGKQL
BOSTA    MQIFVKTLTGKTITLDVEPSDTIENVKTKIQDKEGIPPDQQRLIFAGKQL
SUBDO    MQIFVKTLTGKTITLDVEASDTIENVKTKIQDKEGIPPDQQRLIFAGKQL
ARATH    MQIFVKTLTGKTITLDVESSDTIDNVKTKIQDKEGIPPDQQRLIFAGKQL
ZEAMA    MQIFVKTLTGKTITLDVESSDTIDNVKTKIQDKEGIPPDQQRLIFAGKQL
CHLRE    MQIFVKTLTGKTITLDVESSDTIENVKTKIQDKEGIPPDQQRLIFAGKQL
ASPFU    MQIFVKTLTGKTITLDVESSDTIDNVKTKIQDKEGIPPDQQRLIFAGKQL

NAVPE    EDGRTLSDYNIQKESTLHLVLRLRGG
DROME    EDGRTLSDYNIQKESTLHLVLRLRGG
HOMSA    EDGRTLSDYNIQKESTLHLVLRLRGG
BOSTA    EDGRTLSDYNIQKESTLHLVLRLRGG
SUBDO    EDGRTLSDYNIQKESTLHLVLRLRGG
ARATH    EDGRTLADYNIQKESTLHLVLRLRGG
ZEAMA    EDGRTLADYNIQKESTLHLVLRLRGG
CHLRE    EDGRTLADYNIQKESTLHLVLRLRGG
ASPFU    EDGRTLSDYNIQKESTLHLVLRLRGG
```

Figure 3.1 (A) Genomic sequence of *Navicula pelliculosa* ubiquitin, which has been deposited in GenBank (accession number AY862433). (B) The amino acid sequence of *N. pelliculosa* ubiquitin (NAVPE; AY862433) was aligned with the corresponding sequences from *Drosophila melanogaster* (DROME; M33014.1), *Homo sapiens* (HOMSA; D63791), *Bos taurus* (BOSTA; Z18245.1), *Suberites domuncula* (SUBDO; Y17004.1), *Arabidopsis thaliana* (ARATH; L05917), *Zea mays* (ZEAMA; U29162.1), *Chlamydomonas reinhardtii* (CHLRE; X15427.1) and *Aspergillus fumigatus* (ASPFU; AY817687.1).

proximity of the cell wall, especially at the side of the girdle bands and the cleavage furrow of dividing cells (Fig. 3.2C, D), in line with the suggestion made earlier that the ubiquitination machinery is involved in valve formation.

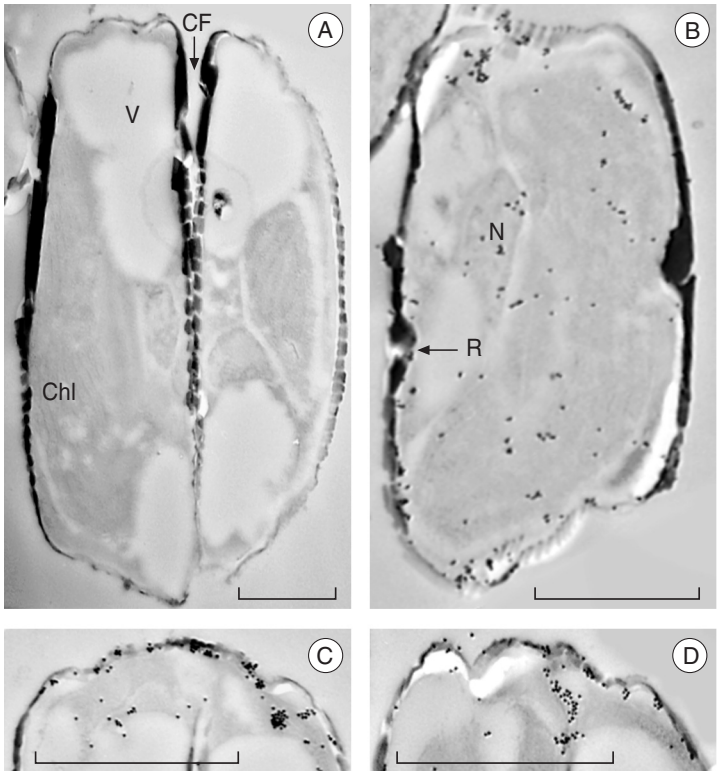

Figure 3.2 Immunocytochemical localization of ubiquitin in cells of *Navicula pelliculosa*. (A) A cross-section of a dividing cell in a control where the primary antibody was omitted. (B) A longitudinal section of a cell, showing the random distribution of gold particles (and thus ubiquitin) over the cell. (C) A higher magnification of the girdle band region of a dividing cell, showing a clear accumulation of ubiquitin in this region. (D) Ubiquitin also appears to accumulate close to the girdle bands and along the cleavage furrow (arrow). Abbreviations: Chl = chloroplast; R = raphe; CF = cleavage furrow; and V = vacuole. The scale bars measures 1 μm.

In both the cell free- and the EDTA-extracts the total protein concentration was in a similar range at all intervals, but the SDS-extracts contained about 6-8 times more protein, with levels ranging between 6.3 and 9.1μg protein/μL. In the course of valve formation the protein concentrations in the cell free extracts remained quite stable in the Si-synchronized cells (Fig. 3.3), whereas the protein concentration in the SDS-extracts somewhat fluctuated during this period. The protein concentration in the EDTA-extracts increased in the first 5 minutes: from 0.7 to 1.3 μg protein/μL. It remained at this level for the next 15 min, whereafter it gradually returned back to the level 0.5 μg protein/μL in the remaining period of valve formation (Fig. 3.3).

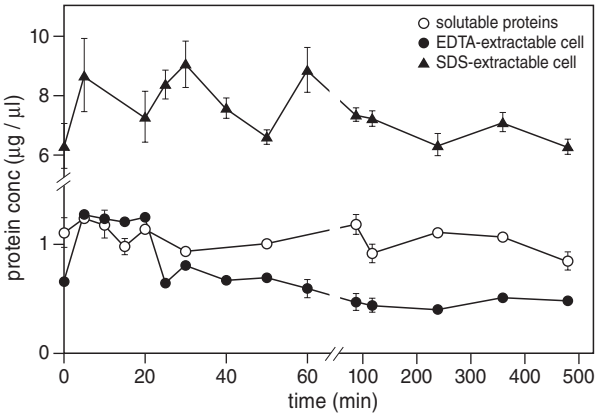

Figure 3.3 Protein levels in the three different extracts obtained during valve formation of Si-synchronized cells of Navicula pelliculosa. The proteins were extracted in the following sequence: soluble proteins referred to as the cell free extracts, EDTA-extractable cell wall-associated proteins, and SDS-extractable cell wall-associated proteins.

Using anti-ubiquitin in Western blotting, the levels of (poly)-ubiquitin and ubiquitinated proteins that were present at every interval were examined in more detail for the 3 extracts. As a positive control ubiquitin from bovine red blood cells was used (data not shown). Only for the identified positively labeled protein bands the labeling intensity was determined by image analysis. The apparent molecular masses of the anti-ubiquitin labeled proteins were estimated using molecular markers (Fig. 3.4, lane 4). In the three different extracts (the cell free-, the EDTA-, and the SDS-extracts) all the positively labeled protein bands were detected at every interval examined (Figs 3.4-7). In the cell free extracts 13 distinct anti-ubiquitin labeled protein bands were detected, varying in mass between 30 and 250 kDa (Fig. 3.4, lane 1). In both the EDTA- and SDS-extracts 6 different proteins were labeled with anti-ubiquitin; their mass ranged from 35-225 kDa and 32-240 kDa, respectively (Fig. 3.4, lane 2 and 3). In addition, free-ubiquitin (8.5 kDa in mass) appeared to be also present in the EDTA-extracts (data not shown); the presence of free ubiquitin served as a control of ubiquitin labeling, but was not included in labeling intensity estimates.

In the cell free extracts a significant positive second-order polynomial correlation was observed between the level of ubiquitinated proteins in the course of valve formation for the proteins with a mass of 110, 98, 95, 80, 70, 45, and 43 kDa (Fig. 3.5A, B, C, D), with r2-values of 0.58, 0.69, 0.81, 0.68, 0.92, 0.51, and 0.74, respectively. For all these proteins the level showed a clear increase in the first stage (120 min) of valve formation followed by a gradual decrease later in the process. Although there was no significant second order polynomial correlation for the protein with a molecular mass of 48 kDa, the labeling intensity of this protein

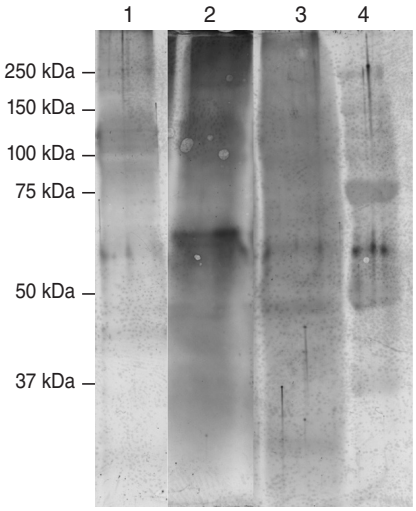

Figure 3.4 Western blots revealing the detection of anti-ubiquitin labeled proteins of one time interval in the cell free-extract (lane 1), EDTA-extract (lane 2), and SDS-extract (lane 3) in Si-synchronized cells of *Navicula pelliculosa*. Lane 4 shows prestained marker proteins.

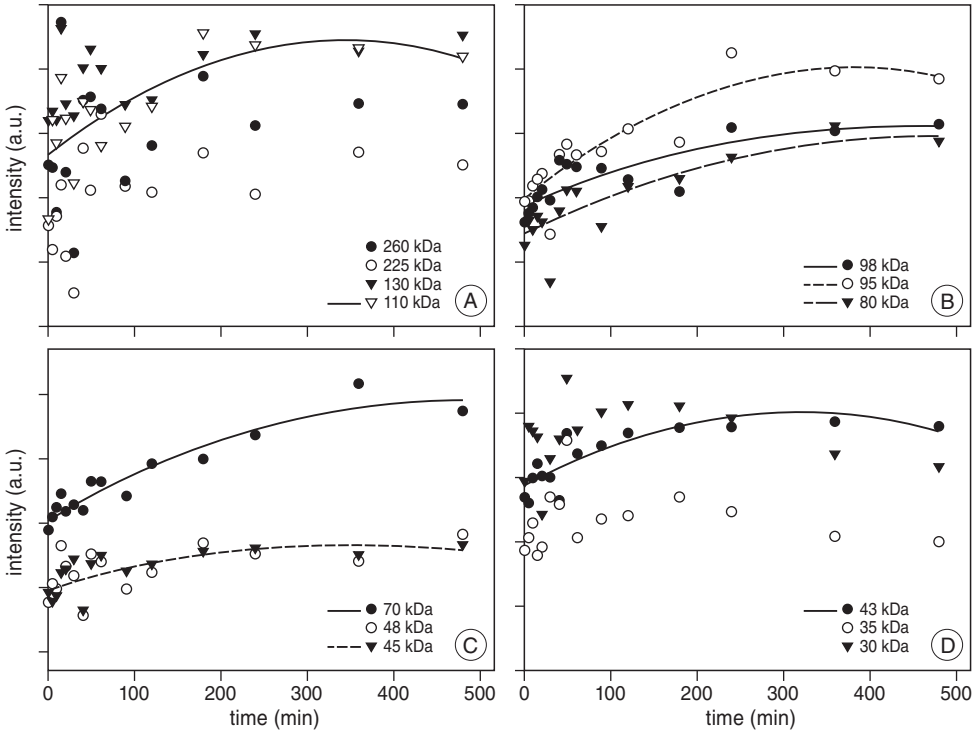

Figure 3.5 Ubiquitin labeling intensity in the course of valve formation of Si-synchronized cells of *Navicula pelliculosa* for the ubiquitinated proteins present in the cell free extracts. The regression lines shown in the graphs represent significant second order polynomial fits. The 13 different proteins positively identified by anti-ubiquitin labeling are discriminated in graphs A-D.

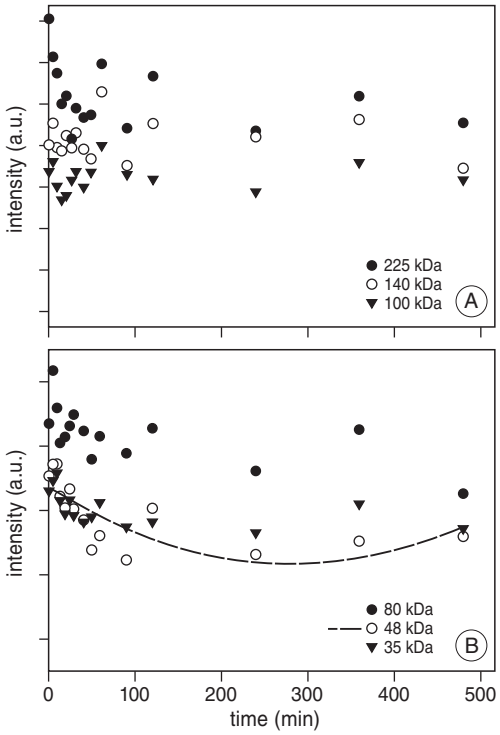

Figure 3.6 Ubiquitin labeling intensity in the course of valve formation of Si-synchronized cells of *Navicula pelliculosa* for the proteins present in the EDTA-extracts. The regression line shown in the graphs represent a significant second order polynomial fit. The 6 different proteins positively identified by anti-ubiquitin labeling are discriminated in graphs A and B.

was significantly lower in the first 60 minutes of valve formation when compared to the following period (Wilcoxon rank sum test, p-value = 0.032).

The labeling intensity of ubiquitinated proteins with masses of 225, 140, 100, 80, and 35 kDa in the EDTA-extracts varied in the course of valve formation (Fig 3.6.A, B). Only for the protein of 48 kDa a significant negative second order polynomial correlation was found ($r^2 = 0.57$), indicating that its level decreases rapidly in the early stage (< 120 min) followed by a gradual increase after 240 min (Fig. 3.6B). Of the other proteins in the EDTA-extracts, only the one with a mass of 35 kDa showed an significantly elevated level in the first 60 min when compared to the later interval (Wilcoxon rank sum test, p-value = 0.017).

In the SDS extracts only 6 proteins appeared to be positively labeled by anti-ubiquitin (Fig. 3.4, lane 3). Again significant positive second order polynomial correlations were observed for the levels of all ubiquitinated proteins in the course of valve formation. For the proteins with masses of 240, 125, 95, 48, 42, and 32 kDa, with r^2-values of 0.57, 0.74, 0.76, 0.61, 0.51, and 0.78, respectively. Typically,

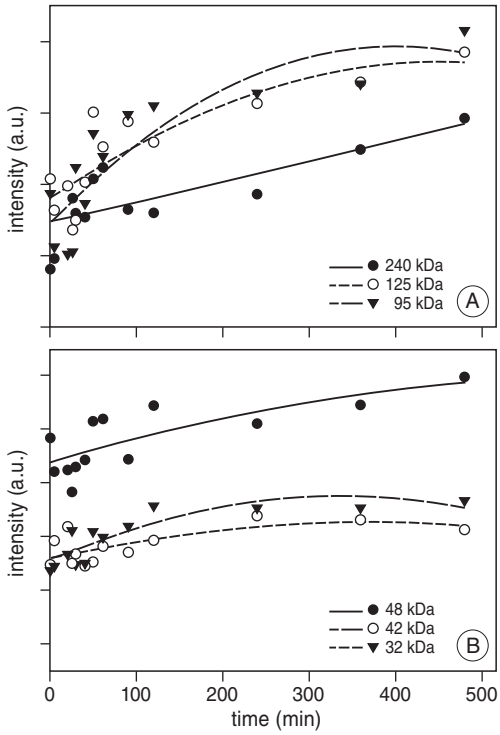

Figure 3.7 Ubiquitin labeling intensity in the course of valve formation of Si-synchronized cells of *Navicula pelliculosa* for the proteins present in the SDS-extracts. The regression line shown in the graphs represent a significant second order polynomial fit. The 6 different proteins positively identified by anti-ubiquitin labeling are discriminated in graphs A and B.

the labeling intensity of all ubiquitinated proteins increased substantially during the first 120 min of valve formation (Fig. 3.7A, B). Thereafter a gradual decrease was detected, except for the 240 kDa protein; its level continued to increase over the whole period of valve formation.

In order to define the relative contribution of all ubiquitinated proteins per extract over the intervals studied, we determined the ratios of the labeling intensity of ubiquitinated proteins as cell free- : EDTA-extracts, as cell free- : SDS-extracts, and as EDTA- : SDS-extracts (Fig. 3.8). The contribution of EDTA-extractable ubiquitinated proteins clearly decreased over those in the cell free extracts (Fig. 3.8A). The changes in cell free- : EDTA-extract ratio in the course of valve formation again fitted a positive second order polynomial correlation ($r^2 = 0.61$); the ratio steeply increased for 120 min, whereafter it leveled off. From the ratios of ubiquitinated proteins in cell free- and SDS-extracts we noticed a slight increased contribution of soluble ubiquitinated proteins (present in the cell free extracts), but this change was not significant. The ratio analysis of EDTA- : SDS-extract indicated

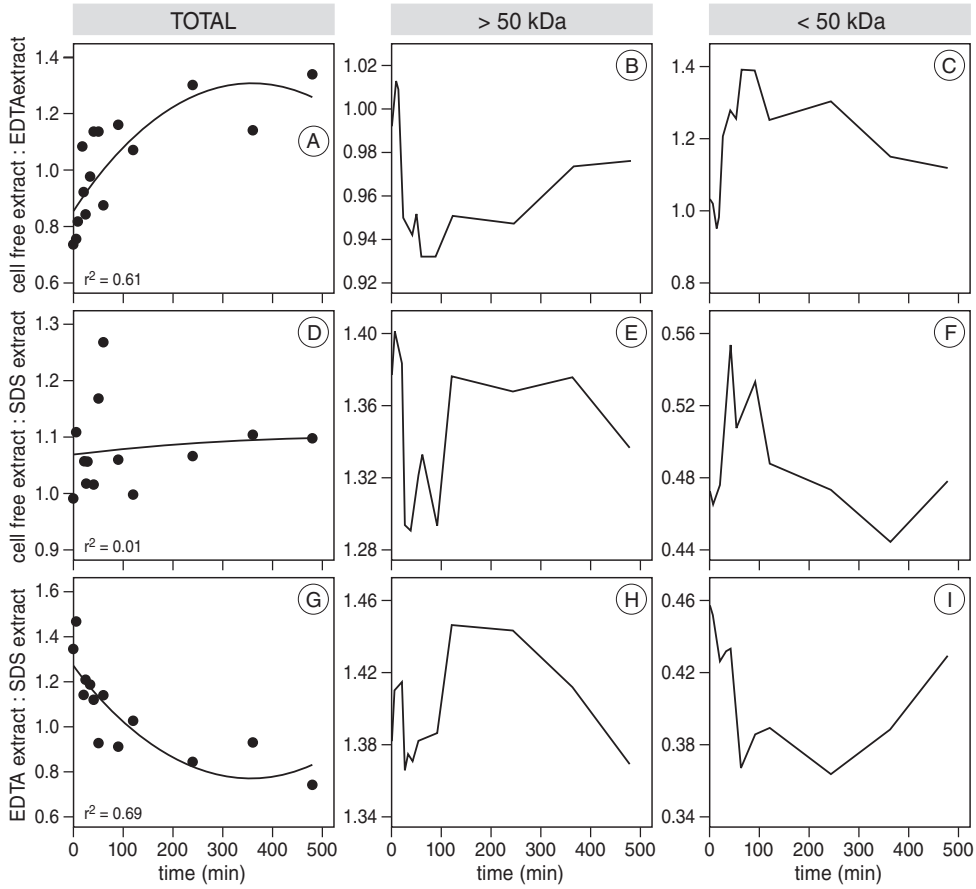

Figure 3.8 Analysis of the relative contribution of ubiquitinated proteins (A,D,G) and a discrimination of smaller (< 50 kDa) and larger (> 50 kDa) protein classes in valve forming Si-synchronized cells of *Navicula pelliculosa*, based on the ratios of their labeling intensities. A, D, and G) ratios including all ubiquitinated proteins as cell free-: EDTA-extracts, cell free-: SDS-extracts, and EDTA-:SDS-extracts, respectively. B, E, and H) ratios including ubiquitinated proteins > 50 kDa as cell free-: EDTA-extracts, cell free-: SDS-extracts, and EDTA-:SDS-extracts, respectively. C, F, and I) ratios including ubiquitinated proteins < 50 kDa as cell free-: EDTA-extracts, cell free-: SDS-extracts, and EDTA-:SDS-extracts, respectively. The lines in graphs A, D, and G represent significant second order polynomial fits.

that ubiquitinated SDS-extractable proteins dominate in later stages of valve formation (> 90 min) with ratio-values that decreased from about 1.2 towards approximately 0.8, which thereafter turned back to the starting value (Fig. 3.8G); in this case regression analysis revealed a negative second order polynomial correlation ($r^2 = 0.69$).

We have also analyzed the aforementioned ratios by discriminating the ubiquitinated proteins in two classes in order to determine the importance of protein size

in the course of valve formation. For this we examined the class of poly-ubiquitin / ubiquitinated proteins with masses < 50 kDa and the other with masses > 50 kDa in more detail. We introduced this size discrimination because small proteins (< 17 kDa) become fully encapsulated during silica formation, whereas larger ones tend to play a role in structure direction processes (Gill & Ballesteros 2000; Vrieling *et al.* 2002). Usually several ubiquitins attach to a target protein prior to degradation and the final mass increased with n * 8.5 kDa. With the notion that the molecular mass of the target protein is ≥ 20 kDa when up to 4 (Pickart 2000; Thrower *et al.* 2000; Weissman 2001) ubiquitin units are subtracted from the ubiquitinated proteins > 50 kDa, we expect that these proteins (minimal 16 kDa in mass) may well play a role in structure direction induced by phase separation (Vrieling *et al.* 2002). Only 4 of all of our identified ubiquitinated proteins have a mass matching that of poly-ubiquitin: the 35 kDa protein present in the cell free- and EDTA-extracts (~ 4 ubiquitins), the 43 kDa protein present in the cell free-extracts, and the 42 kDa protein in the SDS-extracts (each ~ 5 ubiquitins). The molecular masses of the other ubiquitin-labeled proteins appeared not to be a multiplication of free-ubiquitin, and may therefore be considered as ubiquitinated proteins.

Based on our mass discrimination, the cell free- : EDTA-extract ratios revealed that the contribution of larger soluble proteins (> 50 kDa) declined rapidly between 25 and 60 minutes of valve formation (Fig. 3.8B), whereas in the same interval smaller (< 50 kDa) soluble ubiquitinated proteins and/or poly-ubiquitins became more important, judged from their increased ratio (Fig. 3.8C). Beyond 60 min of valve formation the ratios of the large and small protein classes returned to the starting values. The ratio for the > 50 kDa class drops from approximately 1 (equal amount of both protein classes in the cell free- and EDTA-extracts) to 0.93 in the first 60 min, indicating that cell wall-associated EDTA-extractable proteins became important in the very early stage of valve formation and become rapidly targeted for degradation. For the two classes ubiquinated proteins in cell free- : SDS-extracts the ratios revealed a quite similar irregular pattern (Fig. 3.8E, F), as seen for the cell free- : EDTA-extract (Fig. 3.8B, C). For the class of larger ubiquitinated proteins (> 50 kDa), there was a sudden decrease between 0 and 25 min followed by a recovered contribution (Fig. 3.8E). Overall, the contribution of the soluble ubiquitinated proteins was higher over the whole period of valve formation compared to the level of the SDS extractable proteins; the ratio at every interval is > 1. A nearly opposite pattern was observed for the class of ubiquitinated proteins < 50 kDa: a sudden increase until t = 25 min is followed by steady decrease to its starting level (Fig. 3.8F). Over the period of valve formation the contribution of smaller cell wall-associated SDS extractable proteins was always higher than that of the soluble ones; the ratio cell free- : SDS-extracts of proteins < 50 kDa was always < 1.

To discriminate between weakly and strongly cell wall-associated ubiquitinated proteins in the two size classes, the ratios of the EDTA- and SDS-extracts were also

examined (Fig. 3.8H, I). For the proteins > 50 kDa the ratio clearly varied in the course of valve formation; the decline until t = 25 min indicates that the amount of tighter bound SDS-extractable ubiquitinated proteins relatively increased (Fig. 3.8H). The ratio increased between 25 and 120 min, suggesting an elevated relative contribution in favor of EDTA-extractable proteins. In later stages, the stronger cell wall-associated SDS-extractable proteins again became relatively more abundant. At every interval the ratio remained > 1, indicating that the larger EDTA-extractable ubiquitinated proteins (> 50 kDa) were the largest fraction. For the smaller proteins (< 50 kDa), however, the contribution of ubiquitinated proteins is dominated by SDS-extractable ones (at every interval the ratio is < 1). The EDTA : SDS ratio decreases until a transition point at t = 240 min, whereafter it returned to the starting level (Fig. 3.8I).

Discussion

In diatoms, being eukaryotes, it should be expected that the protein degradation machinery as a regular cellular process functions to target short-lived proteins for degradation to the proteasome or lysosome (Hochstrasser 1996; Hershko & Ciechanover 1998; Pickart 2000; Thrower *et al.* 2000; Weissman 2001). We describe here that we identified 25 proteins that labeled with anti-ubiquitin in synchronized cells of *Navicula pelliculosa*. Four of these, with a molecular mass of 35 (2x), 42, and 43 kDa, may well represent poly-ubiquitins; we cannot fully exclude, however, that they are not small ubiquitinated proteins.

The cell wall associated proteins, found in the EDTA- and SDS-extract, are most likely proteins ubiquitinated for degradation, following completion of their task in the process of valve formation. Previously, we identified ubiquitin in *N. pelliculosa*, being specifically located in the proximity of the frustules (Hazelaar *et al.* 2003). Here we confirm this specific location of ubiquitin again by immunocytochemistry (Fig. 3.2) and by demonstrating the specific association of ubiquitinated proteins to the cell walls (Fig. 3.4). Since the sequence of the ubiquitin gene from *N. pelliculosa* is homologous to that of other organisms (Fig. 3.1), we expect that the ubiquitin machinery is also functional in diatoms and may well be involved in valve formation.

The variation in expression of proteins during the cell cycle of *Cylindrotheca fusiformis* has been demonstrated by 2-D electrophoresis of radioactively labeled polypeptides (Okita & Volcani 1980). Also, the expression levels of silicon transporters (SITs; Hildebrand *et al.* 1998) have been studied during cell wall synthesis using RNase protection assays. Their expression is induced prior to the maximal level of silicon incorporation into the cell, each having its own expression pattern during cell wall synthesis. Frustulins that are present in the casing become expressed at later stages of valve formation and in view of their specific location

most likely are required to cover already completed parts of the siliceous frustule elements (van de Poll *et al.* 1999).We cannot fully exclude that some of the cell wall-associated proteins we detected during the present study have their origin in the organic frustule casing. It is known that frustulins remain present in the casing after valve completion and clearly are not degraded. In that perspective, it is of major interest to determine and understand the fate of the proteins associated with the diatom valve in order to predict their spatio- and temporal function in valve micromorphogenesis in the way it was proposed earlier (Vrieling *et al.* 2002).

The fact that the levels of cell wall-associated ubiquitinated proteins, present in the SDS-extract, increased rapidly in the first 120 minutes of valve formation (Fig. 3.7) suggests that these proteins are processed quickly; apparently they are only important in this first period of valve formation. The timing of protein ubiquitination of soluble proteins present in the cell free extracts (Fig. 3.5) is quite similar. The ubiquitination of soluble proteins, however, represents the sum of all cellular events involved in any cellular process of cell growth and division, not specifically valve formation. Of the EDTA-extractable proteins only the level of one protein (with a mass of 48 kDa) showed a significant negative second order polynomial correlation in the course of valve formation. This correlation is the opposite of the positive ones observed for the proteins in both cell free- and SDS-extracts (Fig. 3.6). Possibly this 48 kDa protein is rapidly processed after cytokinesis instead of being essentially involved in valve formation. At present we have not been able to determine the production rates of ubiquitin and its target proteins over the course of valve formation, making it rather difficult to assign ubiquitination events and their regulation exactly to the various stages of valve formation. Based on our data (Fig. 3.5-7), however, it can be stated that the ubiquitination machinery is especially important in the first 120 minutes of valve formation.

The contribution of larger cell wall-associated proteins (> 50 kDa) was changing drastically from a quite steep increase in the first 90 minutes followed by a steady decrease in the remaining period (Fig. 3.8B, E). This suggests that in particular these larger proteins are important in the early stage of valve formation, and, moreover, become rapidly targeted for degradation. For the smaller cell wall-associated proteins (< 50 kDa) the opposite was observed: with an increased contribution in the period > 90 min they function at later stages of valve formation and not in the earliest stages (Fig. 3.8C, F). Based on the class discrimination in the relative contributions of cell wall-associated ubiquitinated proteins (the EDTA- : SDS-extract ratios; Fig. 3.8H, I), also a clear transition was observed within 90 min of valve formation, indicating a ubiquitination event in favor of degradation of larger EDTA-extractable proteins (Fig. 3.8H). Again there was clear difference in protein ubiquitination at the earliest stages (< 90 min) in comparison to the later stages (> 90 min).

The role of proteins and peptides in micromorphogenesis of diatom valves via phase separation processes described by Vrieling *et al.* (2002, 2004), includes the

assumption that protein-rich phases are degraded to leave the pores in the solid amorphous silica. As we now demonstrate, ubiquitin-governed removal may well be the mechanism to achieve this. As judged from the constitutive presence of ubiquitinated cell wall-associated proteins, protein degradation apparently proceeds continuously throughout valve formation (Figs. 3.5-7). This notion agrees with extensive morphological studies, showing that valve formation starts and is completed first at the site around the central nodule and raphe, while continuously growing in the second and third dimension until the final size of the valve has been reached (Pickett-Heaps *et al.* 1990, Round *et al.* 1990). Diatom valve formation relies on controlled expression and degradation of functional proteins; the latter is not a surprise because selective protein degradation is almost always a component of timed regulatory mechanisms that involve timing control (Hochstrasser 1995; 1996). There is obviously a clear difference between the earliest period of valve formation (< 90 min) with respect to protein ubiquitination and the period thereafter, as we have described here, suggesting a well-timed ubiquitination event that correlates to protein turnover at these early stages. This suggestion is supported by the fact that the first hour is an essential stage in the 2-D development of valves, as demonstrated by probing studies (Hazelaar *et al.* 2005); but, 3-D thickening of the valve requires substantially more time. At the time of writing we have not yet distinguished the specific molecular mechanisms of protein ubiquitination and have not characterized the target proteins involved in diatom valve formation. Nevertheless, with the detection of the ubiquitinated cell wall-associated proteins and the correlation of the ubiquitin labeling intensity to different stages of valve formation, we did identify a series of interesting, albeit unknown, proteins that may well play a key role. Our emphasis now will be on the identification and molecular / biochemical characterization of these proteins with the aim to reveal their spatio- and temporal role in valve formation.

Acknowledgements

SH, HS, and EGV were supported by the Technology Foundation STW (grant Gfc4883) applied science division of NWO and the technology program of the Ministry of Economic Affairs, and the European Union (SILIBIOTEC grant QLK3-CT-2002-01967).

References

Altschul, S. F., Gish, W., Miller, W., Myers, E. W. and Lipman, D. J. (1990). Basic local alignment search tool. *J. Mol. Biol.*, 215, 403-410.

Altschul, S. F., Madden, T. L., Schäffer, A. A., Zhang, J., Zhang, Z., Miller, W. and Lipman, D. J. (1997). Gapped BLAST and PSI-BLAST: a new generation of database search programs. *Nucleic Acids Res.*, 25, 3389-3402.

Bradford, M. M. (1976). A rapid and sensitive method for the quantitation of microgram quantities of protein utilizing the principle of protein dye binding. *Anal. Biochem.*, 72, 248-254.

Chenna,R., Sugawara,H., Koike,T., Lopez, R., Gibson, T.J., Higgins, D. G. and Thompson, J. D. (2003). Multiple sequence alignment with the Clustal series of programs. *Nucl. Acids Res.* 31, 3497-3500.

Coombs, J. and Volcani, B. E. (1968). Studies on the biochemistry and fine structure of silica-shell formation in diatoms. Chemical changes in the wall of Navicula pelliculosa during its formation. *Planta*, 82, 280-292.

Gill, I. and Ballesteros, A. (2000). Bioencapsulation within synthetic polymers (Part 1): sol-gel encapsulated biologicals. *TIBTECH*, 18, 282-296.

Gordon, R. and Drum, R. W. (1994). The chemical basis of diatom morphogenesis. *Int. Rev. Cytol.*, 150, 243-372.

Hazelaar, S., van der Strate, H. J., Gieskes, W. W. C. and Vrieling, E. G. (2003). Possible role of ubiquitin in silica biomineralization in diatoms: identification of a homologue with high silica affinity. *Biomol. Engin.*, 20, 163-169.

Hazelaar, S., van der Strate, H. J., Gieskes, W. W. C. and Vrieling, E. G. (2005). Monitoring rapid valve formation in the pennate diatom species *Navicula salinarum* (Bacillariophyceae). *J. Phycol.*,

Hershko, A. and Ciechanover, A. (1998). The ubiquitin system. *Annu. Rev. Biochem.*, 67, 425-479.

Hildebrand, M. (2003). Biological processing of nanostructered silica in diatoms. *Progr. Org. Coatings*, 47, 256-266.

Hildebrand, M., Dahlin, K. and Volcani, B. E. (1998). Characterization of a silicon transporter gene family in *Cylindrotheca fusiformis*: Sequences, expression analysis, and identification of homologs in other diatoms. *Mol. Gen. Genet.*, 260, 480-486.

Hildebrand, M., Volcani, B. E., Gassmann, W. and Schroeder, J. I. (1997). A gene family of silicon transporters. *Nature*, 385, 688-689.

Hochstrasser, M. (1995). Ubiquitin, proteasomes, and regulation of intracellular protein degradation. *Cur. Opin. Cell Biol.*, 7, 215-223.

Hochstrasser, M. (1996). Ubiquitin-dependent protein degradation. *Ann. Rev. Genet.*, 30, 405-439.

Kröger, N., Bergsdorf, C. and Sumper, M. (1994). A new calcium binding glycoprotein family constitutes a major diatom cell wall component. *EMBO J.*, 13, 4676-4683.

Kröger, N., Bergsdorf, C. and Sumper, M. (1996). Frustulins: Domain conservation in a protein family associated with diatom cell walls. *Eur. J. Biochem.*, 239, 259-264.

Kröger, N., Deutzmann, R. and Sumper, M. (1999). Polycationic peptides from diatom biosilica that direct silica nanosphere formation. Science, 286, 1129-1132.

Kröger, N., Lehmann, G., Rachel, R. and Sumper, M. (1997). Characterization of a 200-kDa diatom protein that is specifically associated with a silica-based substructure of the cell wall. *Eur. J. Biochem.*, 250, 99-105.

Kröger, N., Lorenz, S., Brunner, E. and Sumper, M. (2002). Self-assembly of highly phosphorylated silaffins and their function in biosilica morphogenesis. *Science*, 298, 584-586.

Kröger, N. and Wetherbee, R. (2000). Pleuralins are involved in theca differentiation in the diatom *Cylindrotheca fusiformis*. *Protist*, 151, 263-273.

Kyhse-Anderson, J. (1984). Electroblotting of multiple gels: a simple apparatus without buffertank for rapid transfer of proteins from polyacrylamide to nitrocellulose. *J. Biochem. Biophys. Meth.*, 10, 203-209.

Laemmli, U. K. (1970). Cleavage of structural proteins during the assembly of the head of bacteriophage T4. *Nature*, 227, 680-685.

Lowry, O. H., Rosebrough, N. J., Farr, A. L. and Randall, R. J. (1951). Protein measurement with the Folin Phenol Reagent. *J. Biol. Chem*., 193, 265-275.

Müller, W. E. G. (2003). *Silicon biomineralization: Biology, Biochemistry, Molecular Biology, Biotechnology*. Berlin Heidelberg: Springer-Verlag.

Okita, T. W. and Volcani, B. E. (1980). Role of silicon in diatom metabolism. X. Polypeptide labelling patterns during the cell cycle, silicate starvation and recovery in *Cylindrotheca fusiformis. Exp. Cell Res.*, 125, 471-481.

Pickart, C. M. (2000). Ubiquitin in chains. *Trends Biochem. Sci.*, 25, 544-548.

Pickett-Heaps, J. D., Schmid, A. M. M. and Edgar, L. A. (1990). The cell biology of diatom valve formation. *Progr. Phycol. Res.*, 7, 1-168.

Poulsen, N., Sumper, M. and Kröger, N. (2003). Biosilica formation in diatoms: Characterization of native silaffin-2 and its role in silica morphogenesis. *Proc. Natl. Acad. Sci. USA*, 100, 12075-12080.

Reynolds, E. S. (1963). The use of lead citrate at high pH as an electron opaque stain in electron microscopy. *J. Cell Biol*., 17, 208-212.

Round, F. E., Crawford, R. M. and Mann, D. G. (1990). *The diatoms, biology & morphology of the genera*. Cambridge: Cambridge University press.

Slot, J. W. and Geuze, H. J.(1984). Gold markers for single and double immunolabeling of ultrathin cryocsections. In J. M. Polak and I. M. Varndell (Eds) *Immunolabeling for electronmicroscopy* (pp. 129-149). Amsterdam: Elsevier.

Sumper, M. (2002). A phase separation model for the nanopatterning of diatom biosilica. *Science*, 295, 2430-2433.

Sumper, M. and Kröger, N. (2004). Silica formation in diatoms: the function of long-chain polyamines and silaffins. *J. Mater. Chem*., 14, 2059-2065.

Sun, Q., Beelen, T. P. M., Santen van, R. A., Hazelaar, S., Vrieling, E. G. and Gieskes, W. W. C. (2002). PEG-mediated silica pore formation monitored in situ by USAXS and SAXS: systems with properties resembling diatomaceous silica. *J. Phys. Chem*. B, 106, 11539-11548.

Sun, Q., Vrieling, E. G., van Santen, R. A. and Sommerdijk, N. A. J. M. (2004). Bioinspired synthesis of mesoporous silicas. *Curr. Op. Sol. St. Mat. Sci*., 8, 111-120.

Tanaka, K. (1998). Proteasome: structures and biology. J. Biochem., 123, 195-204.

Thamatrakoln, K. and Hildebrand, M. (2005). Approaches for functional characterization of diatom silicic acid transporters. *J. Nanosci. Nanotechnol*., 5.

Thrower, J. S., Hoffman, L., Rechsteiner, M. and Pickart, C. M. (2000). Recognition of the polyubiquitin proteolytic signal. *EMBO J*., 19, 94-102.

van de Poll, W. H., Vrieling, E. G. and Gieskes, W. W. C. (1999). Location and expression of frustulins in the pennate diatoms *Cylindrotheca fusiformis, Navicula pelliculosa*, and *Navicula salinarum* (Bacillariophyceae). *J. Phycol*., 35, 1044-1053.

Veldhuis, M. J. W. and Admiraal, W. (1987). Influence of phosphate depletion on the growth and colony formation of *Phaeocystis pouchetii. Mar. Biol.*, 95, 47-54.

Vierstra, R. D. (1996). Proteolysis in plants: mechanism and functions. *Plant Mol. Biol.*, 32, 275-302.

Vrieling, E. G., Beelen, T. P. M., van Santen, R. A. and Gieskes, W. W. C. (2002). Mesophases of (bio)polymer-silica particles inspire a model for silica biomineralization in diatoms. *Angew. Chem. Int. Ed*., 41, 1543-1546.

Vrieling, E. G., Hazelaar, S., Gieskes, W. W. C., Sun, Q., Beelen, T. P. M. and van Santen, R. A. (2003). Silicon biomineralization: Towards mimicking biogenic silica formation in diatoms. In W. E. G. Müller (Ed) *Silicon biomineralization: Biology, Biochemistry, Molecular Biology, Biotechnology* (pp. 301-334). Berlin Heidelberg: Springer-Verlag.

Vrieling, E. G., Sun, Q., Beelen, T. P. M., Hazelaar, S., Gieskes, W. W. C., van Santen, R. A. and Sommerdijk, N. A. J. M. (2005). Controlled silica synthesis inspired by diatom silicon biomineralization. *J. Nanosci. Nanotechnol.*, 5, 68-78.

Weissman, A. M. (2001). Themes and variations on ubiquitylation. *Nat. Rev. Mol. Cell Biol*., 2, 169-178.

Wong Po Foo, C., Huang, J. and Kaplan, D.L. (2004) Lessons from seashells: silica mineralization via protein templating. *Trends Biotechnol.*, 22, 577-585.